Polyelectrolyte Multilayer Formation on Neutral Hydrophobic Surfaces

Juhyun Park[†] and Paula T. Hammond*[,‡]

Department of Materials Science and Engineering and Department of Chemical Engineering, Massachusetts Institute of Technology, Cambridge, Massachusetts 02139

Received June 3, 2005; Revised Manuscript Received August 27, 2005

ABSTRACT: Pyrene-labeled poly(allylamine hydrochloride) (PAH-Py) has been used to trace the conformational and depletion behaviors of polyelectrolyte chains on neutral hydrophobic Teflon-AF, octadecyltrichlorosilane, or poly(dimethylsiloxane) during assembling by the layer-by-layer deposition technique. The results are used to qualitatively describe how the final quality of multilayer thin films relies on salt stabilization. PAH-Py chains adsorb onto the surfaces in a stretched conformation and form a uniform and dense layer, confirming Dobrynin and Rubinstein's theory. Without an added electrolyte in the polyelectrolyte solutions used for building up multilayers, the PAH-Py layer was seriously depleted, and the extended chains on the surface recoiled during the assembly process, forming coagulated structures of polyelectrolyte complex. In comparison, uniform and flat multilayer thin films were achieved on the surfaces with an added electrolyte, presenting a significant role of salt stabilization on the multilayer.

1. Introduction

The layer-by-layer (LBL) self-assembly technique normally involves the sequential adsorption of a polycation/polyanion pair onto a charged substrate. Because of the extreme versatility and convenience of the technique, the applications of LBL assembled polyelectrolyte multilayers have multiplied since Decher and Hong reported LBL multilayers in 1991.[1,2] The advantages of the technique have since triggered many experimental and theoretical studies regarding multilayer properties, which have also opened up new applications, including electrooptic,[3,4] electronic,[5,6] display,[7−9] eletrochromic,[10−13] micropower,[14−16] biosensor devices,[17−20] and drug delivery.[21,22]

Of specific interest in this paper is the formation of polyelectrolyte multilayers on neutral hydrophobic surfaces, a topic that has not been highlighted in the LBL multilayer community, although it is critical in various applications of LBL thin films formed at liquid/solid interfaces involving a noncharged, nonpolar hydrophobic surface. As a particular example of such applications, multilayer transfer printing (MTP) after building up multilayers on a micropatterned poly(dimethylsiloxane) (PDMS) stamp[23] suggests a unique way for patterning multilayer nanocomposite thin films of multiple components in both two and three dimensions. Multilayering of polyelectrolytes on a neutral hydrophobic surface is also a unique and useful way to prepare free-standing LBL thin films for numerous important applications such as batteries,[24] composite films with high mechanical properties,[25] virus-arrayed thin films,[26] membrane coatings,[27−29] the coating of microfluidic devices, optical fibers, and other common surfaces. Furthermore, the mechanical properties of LBL thin films that dramatically affect cell function on polyelectrolyte multilayer biomaterial surfaces can be easily measured using a strain-induced elastic buckling technique when they are assembled on neutral PDMS substrates.[30] However, it presents a unique challenge, and its mechanism has not yet been fully described. It is much more common to observe the layering of polyelectrolytes on plasma-treated PDMS or similar charged surfaces. Only a few papers have actually reported that LBL thin film formation on a neutral hydrophobic surface is possible under certain experimental conditions, but a fundamental understanding of the phenomena has yet to be provided.[31−33]

In this paper, we report the adsorption behavior of a hydrophobic weak polyelectrolyte, poly(allylamine hydrochloride) (PAH), on neutral hydrophobic surfaces such as poly(tetrafluoroethylene-*co*-2,2-bis(trifluoromethyl)-4,5-difluoro-1,3-dioxole) (Teflon-AF), octadecyltrichlorosilane (OTS), and PDMS and the properties of multilayers assembled on the adsorbed PAH layer. To understand the molecular basis of the adhesion properties of the PAH layer, we refer to a scaling theory developed by Dobrynin and Rubinstein[34−38] and use pyrene-labeled PAH chains to calculate a coiling index (the excimer-to-monomer emission ratio in fluorescence spectra, I_E/I_M)[39−44] to trace changes in PAH chain conformation. The assembled multilayer properties that are subject to LBL assembly parameters such as polyion composition, pH, and ionic strength for the adsorption and rinsing steps were studied using spectroscopic ellipsometry, quartz crystal microbalance (QCM), and atomic force microscopy (AFM) techniques. The representative polyion pairs chosen for assembly atop the PAH base layer included a weak polycation, poly(allylamine hydrochloride) (PAH), with a weak polyanion, poly(acrylic acid) (PAA), and a strong polycation, poly(diallyldimethylammonium chloride) (PDAC), with a strong polyanion, poly(sodium 4-styrenesulfonate) (SPS).

2. Experimental Section

2.1. Materials. PAH (M_n = 70K), PDAC (M_n = 100K−200K), SPS (M_n = 70K, polydispersity index (PDI) = 10.5), 1-pyrenecarboxaldehyde, sodium cyanoborohydride ($NaBH_3CN$), OTS, and hexamethyldisilazane (HMDS) were purchased from Aldrich Chemical. PAA (M_n = 90K, PDI = 6.2) was purchased from Polysciences Inc., and Sylguard 184 was

[†] Department of Materials Science and Engineering.
[‡] Department of Chemical Engineering.
* To whom correspondence should be addressed: e-mail hammond@mit.edu.

10.1021/ma051158c CCC: $30.25
Published on Web 11/12/2005

acquired from Dow Chemical. Teflon-AF 2400 (1 wt % solution) was obtained from DuPont Fluoroproducts. All chemicals were used as received. Silicon wafers coated with a thermally oxidized SiO_2 layer (~280 nm) were obtained from Silicon Quest International.

2.2. Synthesis of PAH-Py. A small portion of primary amines in PAH chains was substituted by pyrene via a reductive reaction with 1-pyrenecarboxaldehyde and sodium cyanoborohydride ($NaBH_3CN$) in a solvent mixture of water and methanol (20:80) at pH 6.0 following a literature procedure.[40] To recover products from the reaction mixture, excess chloroform was added, which resulted in a phase separation between an aqueous and an organic phase. The water phase was separated and poured into hydrogen chloride-saturated methanol. Precipitates were collected, dissolved in water, reprecipitated twice into HCl-saturated methanol, and finally dried in a vacuum at room temperature for 24 h. In two batches, pyrene substitution levels of 1 mol % (PAH-Py1, 74% yield) and 0.86 mol % (PAH-Py2, 64% yield) on the PAH were achieved, as determined by UV adsorption spectra (calculated using $\epsilon_{344} = 39\,800\ L^{-1}\ cm^{-1}$).[40]

2.3. Preparation of Neutral Hydrophobic Surfaces. In this work, three neutral hydrophobic substrates were employed: Teflon-AF- and OTS-coated silicon wafers and PDMS sheets.

Teflon-AF. Teflon-AF was coated onto silicon wafers with a thermally oxidized SiO_2 layer after degreasing using sonication in chloroform for 10 min and cleaning under plasma (100 W, oxygen, 0.1−0.5 Torr, 10 min). To increase adhesion between the wafers and Teflon-AF layer, the plasma-treated wafers were first reacted with HMDS vapor in a desiccator for 16 h and cured at 150 °C for 2 h. Teflon-AF was spin-coated on the wafers at 3000 rpm for 30 s and cured at 150 °C for 5 h.

OTS Monolayers: After degreasing and oxygen plasma cleaning, silicon wafers were chemically oxidized for 10 min by immersing the wafers into a freshly prepared mixture of 70% sulfuric acid−30% aqueous solution of hydrogen peroxide (at 30% H_2O_2) at 80 °C, followed by thorough rinsing with deionized water. Immediately after one additional dry oxidation step using oxygen plasma, the wafers were immersed into a reaction mixture of hexadecane (70 mL), tetrachlorocarbon (30 mL), and OTS (1 mM) that was prepared in an inert atmosphere. The reaction time was 1 h, and temperature of the reaction bath was controlled below 10 °C. After the reaction, the substrates were sonicated in chloroform for 5 min to remove excess materials and then postcured for 2 h at 150 °C. The resulting water contact angle of the wafer surface was around 109°, which is similar to that of a PDMS surface.

PDMS. PDMS sheets were prepared by curing Sylguard 184 on a silicon wafer for 12 h at 60 °C, followed by removal from the silicon surface.

2.4. PAH-Py Adsorption and PEM Assembly. PAH-Py was dissolved in deionized water, and the pH was adjusted by titrating HCl or NaOH. For adsorption experiments, wafers coated with Teflon-AF or OTS or PDMS sheets were immersed into the PAH-Py solutions in various conditions for 30 min and dried under nitrogen. Polyelectrolyte multilayers were assembled upon the PAH-Py layer utilizing an HMS programmable slide stainer (Zeiss, Inc.). 10 mM (based on the molecular repeat unit of the polymer, ~0.1 wt %) polyelectrolyte solutions were prepared with 18.2 MΩ Millipore water and were pH-adjusted with HCl or NaOH. The hydrophobic substrates with adsorbed PAH were first submerged into the polyanion solutions (PAA or SPS) for 15 min and then taken through a series of three rinse baths of water for 1 min each. Afterward, the slides were immersed in the polycation solutions (PAH or PDAC) for 15 min, followed by the same rinsing procedure.

2.5. Measurements. Fluorescence spectra were obtained using a SPEX Fluorolog 3 spectrometer and a DM3000F detector at room temperature. The emission wavelength for excitation spectra was 377 nm for monomer excitation and 495 nm for excimer excitation, and the excitation wavelength for emission spectra was 343 nm. All spectra were uncorrected. The slits were set at 0.3 mm for solution samples to avoid fluorescence saturation, keeping the maximum photon count below an order of 10^6, whereas they were set at 2 mm for substrate samples. The coiling index was calculated by dividing the integrated fluorescence intensity from the excimers (I_E, 450−650 nm) by that from pyrene monomers (I_M, 370−400 nm).[40]

Multiple-wavelength ellipsometric measurements were performed on a spectroscopic ellipsometer (model M-44, J. A. Woollam Co., Inc., Lincoln, NE) aligned at an incidence angle 70° from the surface normal. Four measurements were obtained for each sample and averaged. To reduce noise, 100 revolutions of the analyzer were accumulated. Thickness was calculated using a four-layer model of Si, SiO_2, Teflon-AF, and polyelectrolyte layers. Optical constants of the SiO_2 and Teflon-AF layers obtained from manufacturers were used. Modeling and thickness calculations were carried out using the WVASE software from J.A. Woollam Co.

The topography of substrate surfaces was monitored using a Veeco Nanoscope IV scanning probe microscope (Santa Barbara, CA) in tapping mode with a silicon etched tip.

During assembling multilayers, QCM was measured using a home-built device, and the resonance frequency shift, ΔF, of the QCM was calculated. The gold surface of the QCM electrode was modified to a hydrophobic surface by reacting with a 2 mM dodecyl thiol solution in hexane. The resonance frequency of the QCM electrode was 10 MHz.

3. Results and Discussion

3.1. Characterization of PAH-Py in Solutions. 3.1.1. Fluorescence Characteristics. When pyrene groups attached to PAH chains associate due to variations in chain conformations, the fluorescence intensity from preassociated pyrenes (static excimers) drastically increases and that from isolated ones (monomer) decreases. Because the static excimers are formed when two pyrene groups are within close distance (4−5 Å) of each other in the excited state, the coiling index, derived from the ratio of the fluorescence intensities from these two states, can serve as an indicator of chain conformational variations during PAH monolayer adsorption and multilayer assembly processes and provide useful information about PAH adsorption behavior. Excimer formation can take place via either a dynamic or static mechanism, whereas the coiling index is only valid when calculated from static excimers. Dynamic excimers are formed when isolated pyrenes are first excited by light and then interact with other pyrenes in the electronic ground state. In comparison, static excimers are formed when preassociated pyrene dimers or aggregates are directly excited, for which the calculated coiling index becomes meaningful when determining adsorption behavior. To detect whether pyrene groups are preassociated, we used two photophysical parameters:[40,41] the shift in the wavelength maxima and the peak-to-valley ratio of the (0,0) transition in the excitation spectra. Excitation spectra were viewed at the monomer emission ($\lambda_{emission} = 377$ nm) and at the excimer emission ($\lambda_{emission} = 495$ nm) for 0.1 wt % PAH-Py solutions from pH 3.5 to 10.5. It was observed that the wavelength maxima of the (0,0) transition in the excimer spectra was significantly red-shifted by 6 and 8 nm for the 0.1 wt % PAH-Py1 (10.37 mM polymer solution, 1 mol % pyrene substitution) and PAH-Py2 (10.49 mM polymer solution, 0.86 mol % pyrene substitution) solutions, respectively, compared to that in the monomer excitation. The peak-to-valley ratio for the (0,0) transition of the monomer and excimer spectra, P_M and P_E ($P_M = I_M^{peak}/I_M^{valley}$ for the monomer and $P_E = I_E^{peak}/I_E^{valley}$ for the excimer), of PAH-Py1 solutions were 1.76 and 1.27, and those of PAH-Py2 solutions were 1.53 and 1.40,

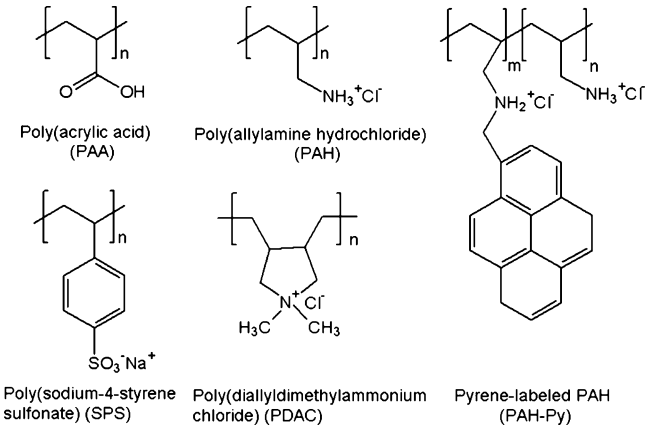

Figure 1. Chemical structures of polyelectrolytes.

respectively. Excitation spectra at 377 and 495 nm of a representative solution, containing 0.1 wt % PAH-Py2 at pH 6.14, are shown in the Supporting Information. These results indicate that excimers are formed via a static mechanism in these experiments.

3.1.2. PAH Chain Conformation in Solution. The chain conformations of PAH-Py in solution are dependent on ionic strength and the degree of ionization as controlled by solution pH. As theoretically and experimentally demonstrated in the literature,[38,45−47] when the chains are fully charged, they assume a stretched conformation because of electrostatic repulsion between charged groups on the chains. Decreasing the degree of ionization of the polymer chains by increasing pH or shielding electrostatic repulsion with added electrolytes increases the short-range attractions between uncharged groups, inducing a partial collapse of the chains due to a Rayleigh instability.[38] The resulting chain conformation is analogous to a pearl necklace structure in which extended strings connect collapsed spherical beads to each other. As the degree of ionization decreases or ionic strength increases, the conformation of polyelectrolyte chains abruptly transitions from necklace to spherical globule shapes with different numbers of beads.[38]

The coiling index of PAH-Py reflects the conformational behavior related to pH and solution concentrations. As explicitly shown in Figure 2a, the fluorescence spectra change significantly with solution pH, confirming that the coiling index calculated from the spectra can be a useful indicator of chain conformations. In general, the coiling index of PAH-Py increases with pH, indicating increasing pyrene-association due to conformational transitions. The degree of ionization of PAH-Py can also be evaluated from the variation of the coiling index and the maxima of excimer peaks in emission spectra. In Figure 2b, two curves cross at pH 8.56, which seems to be in agreement with the pK_a values obtained from potentiometric titration (Supporting Information 2 and Figure S2), as known in the literature.[42,44]

In addition to the pH and ionic strength effects on the coiling index, solution concentration significantly influences the pyrene association. Figure 3 shows the variation of the coiling index with concentration at pH 3.5 and 8.5. In general, the coiling index increases with concentration and shows a transition in the center of the concentration range at each pH. This transition below 0.1 wt % (about 10 mM on a repeat unit basis) is likely to be related to the critical concentration for chain overlapping. As concentrations approach the critical

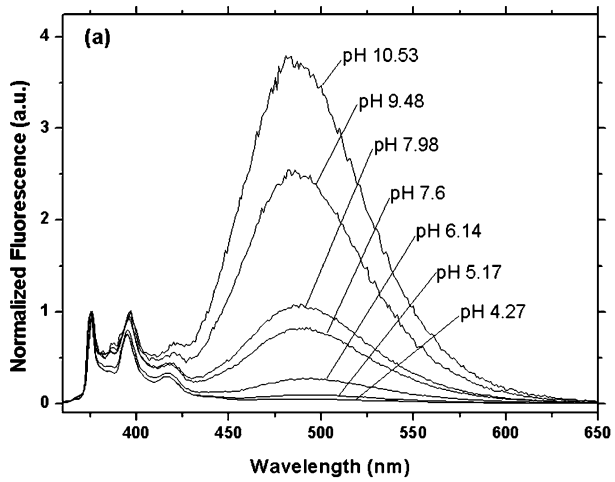

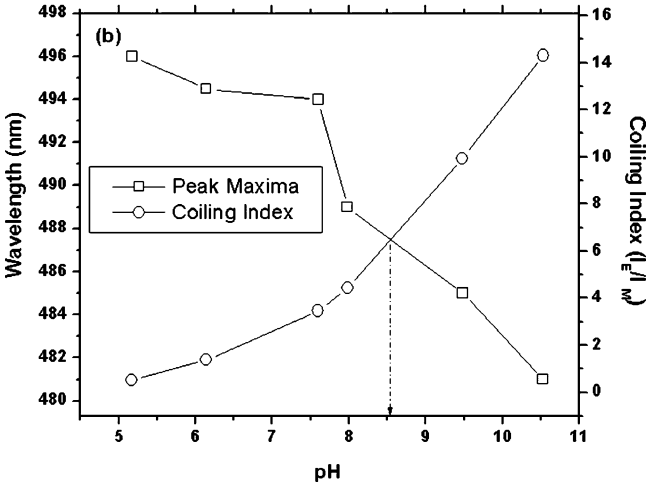

Figure 2. (a) Fluorescence spectra normalized to the intensity of the (0, 0) transition at 377 nm at various pH values and (b) coiling index and maximum excimer peak positions of 0.1 wt % PAH-Py2 solutions varying with solution pH.

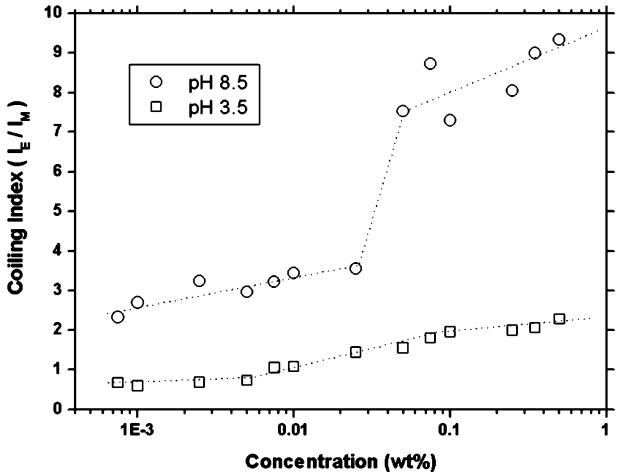

Figure 3. Coiling index variation of PAH-Py1 with solution pH and concentrations.

concentration, interpolymeric pyrene association will increase. Thus, pyrene association primarily originates from intrapolymeric association in the dilute regime and begins to reflect both inter- and intramolecular association beyond the critical concentration. The transition occurs over a broader concentration range at pH 3.5 than at pH 8.5, which is the result of a more stretched chain conformation at pH 3.5. This result is in agreement with dynamic light scattering data where hydro-

dynamic diameters of PAH chains (the same PAH used in this study) fluctuate broadly from 33 to 44 nm at pH 3.5 but are nearly constant at 12 ± 2 nm at pH 8.5.[48] This large fluctuation observed at low pH and high degree of ionization reflects a hydrated, expanded, and nonspherical PAH chain conformation, as the calculation of hydrodynamic diameter is based on the assumption of a spherical particle. Critical concentrations roughly estimated from the radius of gyration measured by static light scattering (15.5 ± 1 nm at pH 3.5 and 7 ± 0.5 nm at pH 8.5)[48] correspond with these transition ranges.

3.2. Adsorption of PAH-Py on Neutral Hydrophobic Surfaces. 3.2.1. Adsorption Theory of Hydrophobic Polyelectrolytes at Neutral Hydrophobic Surfaces. The adsorption of polyelectrolyte chains has typically been studied on charged surfaces. Among theoretical models used to address the adsorption, the Dobrynin and Rubinstein theory (the DR theory)[34−38] provides a useful basis for describing adsorption behavior of hydrophobic polyelectrolytes on neutral hydrophobic surfaces. We simplify the theory to make it applicable to our system and use it to explain the adsorption behavior of PAH-Py.

The important forces governing the adsorption in this study are short-range attractions (van der Waals interactions) between polyelectrolytes or between the polyelectrolytes and surfaces and long-range repulsions between polyelectrolytes. We do not consider other interactions, such as electrostatic attraction, other than short-range attractions of the polyelectrolytes to the surfaces. During adsorption, hydrophobic polyelectrolyte chains can be arranged on the hydrophobic surfaces in an extended conformation due to attractive short-range interactions with the substrate. However, when repulsive interactions between chains are dominant, polyelectrolytes experience an electrostatic barrier as they are adsorbing to the surfaces, resulting in chains that are placed on the surface at a certain distance from each other. In the DR theory, the structure of the adsorption layer is uniquely described using Wigner−Seitz cells, at the center of which the polyelectrolyte chains are localized.

The Wigner−Seitz cell size ξ physically represents the distance between adsorbed chains. The equation for the cell size (Supporting Information 3) indicates that the distance between adsorbed chains is controlled by the electrostatic repulsion between chains and their nonelectrostatic attraction to the adsorbing surface. The cell size ξ scales linearly with the Debye length r_D and the fraction of charged monomers or degree of ionization f, as is also connoted in the original DR theory.

The theory predicts that at a large Debye length, or a large fraction of charged segments, polymer chains adsorb on the surface at great distances from each other. As the Debye length or the fraction of charged monomers decreases, the distance between adsorbed chains decreases, and below a certain value of the Debye length or the fraction of charged monomers, adsorbed chains overlap to form either a monolayer or a 3-D adsorbed layer. In the adsorbed layers of these latter regimes, chains can densely and uniformly adsorb on the surface based on the affinity of the polyelectrolytes for the surface and play a role as the priming layer for the buildup of polyelectrolyte multilayer thin films.

Increasing ionic strength by salt addition plays a paramount role in the adsorption behavior. The theory states that with decreasing Debye length of the hydrophobic moiety, or backbone of the polymer, the chains experience more attractive forces to the surface due to strong short-range dispersion interactions as well as the decreased distance between adsorbed chains. As previously reported,[36,49−51] salt addition can result in the decrease of the adsorbed layer thickness by spreading out the adsorbed chains onto the surface due to the increased attraction.

The final adsorption behavior to be addressed is the depletion of the adsorbed layer. The above theory is only valid under the assumption that short-range attractions to the surface are stronger than solvating forces. However, in the LBL assembly process, adsorbed chains are exposed to various aqueous media conditions during the adsorption and rinse cycles, during which the chains might rearrange or undergo desorption on exposure to changes in ionic strength or degree of ionization or via the formation of ionic complexes in solution with counter polyelectrolytes. The quality of multilayers that are built up on this first priming layer significantly depends on this behavior.

On the basis of the above theory, we chose PAH, a hydrophobic weak polyelectrolyte, as the initial polyion for investigation of the adsorption behavior of a hydrophobic polyelectrolyte "base" or primer monolayer and the subsequent multilayer formation atop the primer layer. The fraction of charged monomers for PAH can readily be controlled by adjusting solution pH; thus, we can maximize the adsorption of PAH by varying both variables of ionic strength and degree of ionization to gain a stable base layer for multilayer buildup on a hydrophobic surface. Weak hydrophobic polyelectrolytes can possess a smaller Wigner−Seitz cell size than strong hydrophobic polyelectrolytes by adjusting both pH and ionic strength of solutions during adsorption, causing denser and more uniform adsorption layers.

3.2.2. Coiling Index Variation of PAH-Py after Adsorption. The surfaces of silicon wafers coated with OTS contain closely packed methyl groups that resemble those found in cured PDMS, yielding low surface tensions. The experimental water contact angle value of 109° for OTS implies a surface tension of 21 mN/m, which is a similar value to that of PDMS. Thus, OTS-coated silicon wafers were used as model surfaces in measuring fluorescence spectra of adsorbed PAH-Py. Teflon-AF provides a more hydrophobic surface than OTS and PDMS. Because of its high glass transition temperature and chemical inertness, Teflon-AF-coated surfaces should also be more stable than OTS-coated surfaces in the presence of a range of aqueous media. After spin-coating, the resulting static water contact angle of the surface was around 120°, the film thickness was in the range 95−110 nm, and the surface roughness was 0.51 ± 0.03 nm.

The conformational variation of PAH-Py chains after adsorption can clearly be demonstrated by comparing the coiling index in solution to that after adsorption. All adsorption experiments were carried out using 0.1 wt % PAH-Py solutions, which was ~10 mM on a repeat unit basis, a typically used concentration in LBL assemblies. Because conformations of weak polyelectrolytes are affected by both ionic strength and the degree of ionization, we first adsorbed the chains at relatively constant ionic strength while changing the degree of ionization with pH adjustment. Figure 4 shows the change of the coiling index with pH before and after

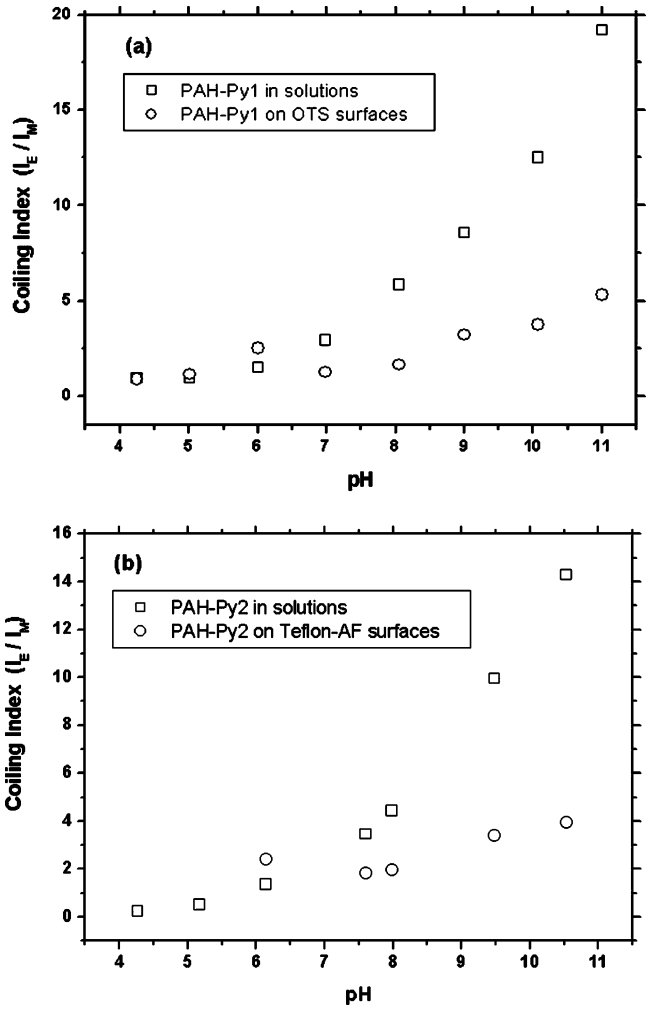

Figure 4. Coiling index variation of (a) PAH-Py1 on OTS surfaces and (b) PAH-Py2 on Teflon-AF surfaces before (square) and after (circle) adsorption. Concentration of all solutions was fixed at 0.1 wt %, and the adsorption time was 30 min.

adsorption onto the neutral hydrophobic OTS and Teflon-AF surfaces. In solution, the coiling index does not show any significant change up to pH 6 but increases markedly after pH 8. This result suggests that below pH 6 the chain is in an extended conformation due to electrostatic repulsion between charged groups on the polymer chain. Over pH 8, we observe that chain conformation abruptly changes, possibly from an extended chain to necklace or more globular shapes. These results support the abrupt change in the radius of gyration of PAH chains with pH. The R_g of PAH was 16 ± 2 nm below pH 6 but drastically decreased to 7 ± 1 nm above pH 6−9, indicating conformational transitions with solution pH.[48]

For the polyions adsorbed to the surfaces, the coiling index above pH 8 was much lower than in solution. Total adsorbed amounts of PAH-Py increased with increasing pH, as measured experimentally by integrating the total number of photons in uncorrected fluorescence spectra from 350 to 650 nm. In the lower pH regime, the coiling index of the adsorbed chains did not vary largely from that in solution. These results agree well with theoretical predictions that hydrophobic polyelectrolytes are arranged on hydrophobic surfaces in stretched chain conformations due to short-range interactions. In the low-pH region, chains are already extended in solution, so there is expectedly less change in coiling index during adsorption. However, the decrease in coiling index after adsorption from high pH, and thus the more stretched arrangement of chains on the surface, is remarkable considering that the chains in solution have compact spherical conformations in the high-pH regime due to low degrees of ionization.

Adsorption relies on hydrophobic interactions between the surface and the hydrophobic backbone of PAH-Py, and the increased fraction of charged groups in the low-pH region results in strong repulsion between PAH-Py segments following adsorption to the hydrophobic surfaces. As a result, PAH-Py solutions would completely dewet from the surface when the substrates were taken out of solution, indicating that the chain adsorption might be dilute or semidilute, and a wettable charged uniform monolayer was not formed. Ellipsometry data in this region also suggest that the adsorbed layer is not optically uniform. On the other hand, the chains are strongly adsorbed onto the surface above pH 8 due to the loss of repulsive groups along the backbone and enhanced hydrophobic interactions, thus resulting in a wettable surface. The coiling index in this range increases slightly with pH but shows a much smaller value than that measured in solution.

Above pH 8, variation in both adsorbed chain concentrations and conformations on surfaces can contribute to the coiling index. To investigate both contributions and the effect of varying ionic strength, PAH-Py2 was adsorbed onto Teflon-AF surfaces from solutions at pH 9.0 with different amounts of added NaCl salt, and the resulting coiling index and adsorbed layer thickness were measured (Figure 5a). In solution, the coiling index increases with added salt, showing that chains are more compactly coiled due to shielding of long-range repulsions with increased ionic strength. Again, this behavior is suppressed dramatically after adsorption on the surface, indicating more extended chains on the surface.

The thickness of the adsorbed layer decreases with ionic strength, although the adsorbed amounts evaluated from the integrated photon counts increase with ionic strength. This thickness change combined with the coiling index provides useful information about the adsorption mechanism. At the lowest salt concentration at pH 9, the thickness is the largest, 4.76 nm, and the coiling index decreases from 6.7 in solution to 3.19 on the surface. Although it is largely decreased, the coiling index on the surface is not due to more extended chain conformations, which would yield a coiling index of around one. These results indicate that the polymer chains might be adsorbed in a perturbed spherical shape, or in a less extended conformation, and that the relatively high coiling index might originate from the contribution of intrapolymeric pyrene association. As the salt concentration increases, both thickness and coiling index decrease. In the extreme condition of the largest salt concentration, the thickness is the lowest value, 2.53 nm, and the coiling index again increases to 3.07. The decrease in thickness shows that increasing ionic strength increases the attractive force to the surface, spreading polymer chains onto the surface. The increased coiling index at 0.5 M NaCl may originate from the contribution of interpolymeric pyrene association in a more densely packed adsorption layer. The change in density of polymer chains implies that the thicker layers are loosely packed and become much more compact at higher ionic strength. This possible mechanism appears

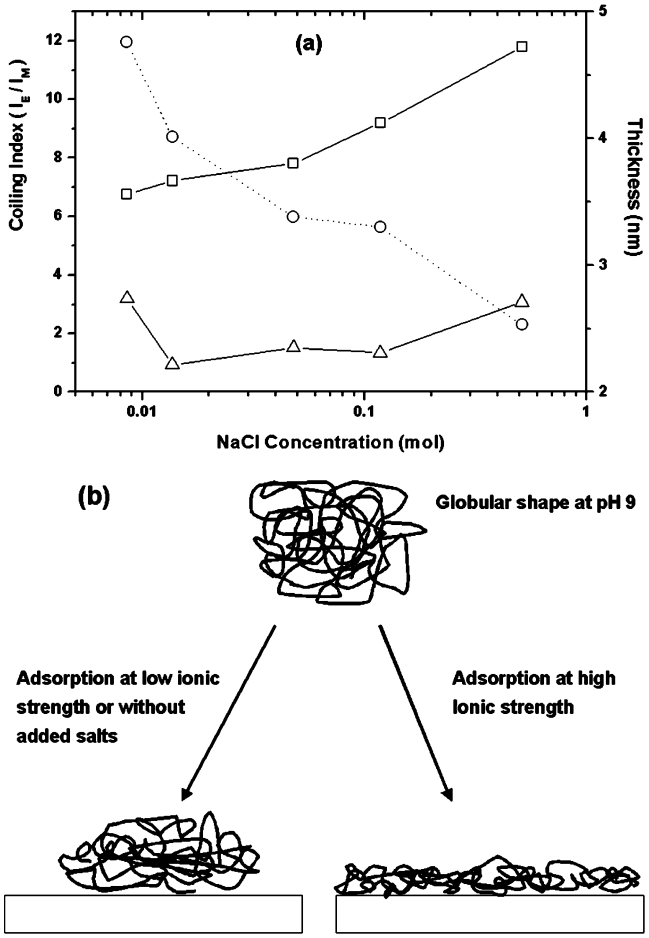

Figure 5. (a) Coiling index variation of PAH-Py2 before (square) and after (triangle) adsorption onto Teflon-AF surfaces at pH 9 with varying added salt concentration, and thickness variation of monolayer (circle) (b) a schematic illustration of an adsorption mechanism.

in theories and is experimentally demonstrated in this study, as schematically illustrated in Figure 5b.

3.3. Polyelectrolyte Multilayers Assembled on Neutral Hydrophobic Surfaces. 3.3.1. Salt Stabilization of the PAH-Py Layer during Multilayer Assembly. The stability of the adsorbed PAH-Py chains during subsequent adsorption and rinsing steps in the LBL assembly process is of paramount interest for building up multilayers upon the primary layer. Variation of solvating power, due to different solution pH and ionic strengths, relatively weak hydrophobic interactions between the hydrophobic surface and the polymer, and a strong tendency to form ionic complexes in solution could cause severe desorption of the adsorbed chains or wrinkling of the adsorbed layer. As first shown by Poncet et. al.,[50] the adsorbed layer of a hydrophobic polyanion, hydrophobically modified PAA, was stabilized when treated by rinsing solutions with increased ionic strength. The mechanism of this stabilization was described by measuring the coiling index under various adsorption conditions and by using in-situ ellipsometry. Their results showed that the adsorbed layer was completely depleted when rinsed by water without added salt but remained as a stable adsorption layer when treated with a rinse solution with added salt. In our study using a hydrophobic polycation, PAH-Py, we further traced the stability of the prime PAH-Py layer during the LBL assembly process and related it to the multilayer quality after the process.

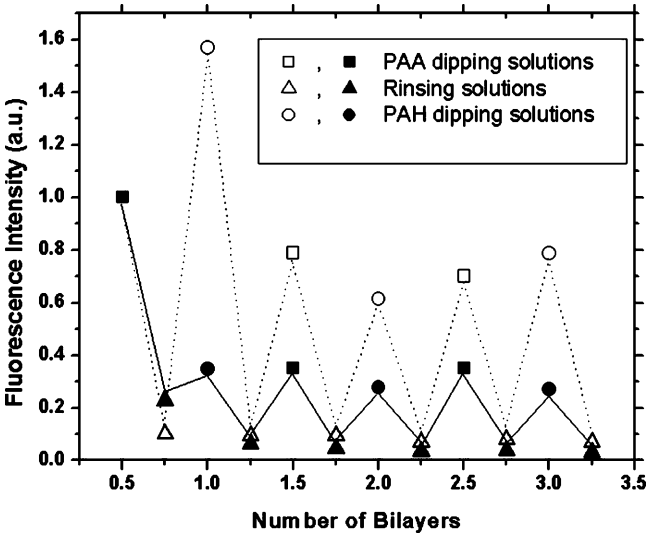

Figure 6. Relative amount of depleted PAH-Py1 chains during assembly process in the case of no added salt in the adsorption solutions (open symbols) and when 0.1 M NaCl was added in the adsorption solutions (filled symbols). PAH-Py1 was adsorbed at pH 9, and the solution pH of all subsequent adsorption solutions of PAH and PAA was fixed at pH 6.5.

The relative amount of depleted PAH-Py lost from the surface in each step of the process was evaluated by measuring the fluorescence spectra of the adsorption and rinsing solutions, which were kept at constant volumes, and measuring the coiling index of PAH at different steps in the process. The salt stabilization effect during the multilayer assembly process for two PAH-Py1/$(PAA/PAH)_3$ films was investigated by changing ionic strength between samples. It should be noted that the labeled PAH was used only for the first adhesion layer. 0.1 M NaCl was used in the construction of one multilayer sample and excluded in the other, and rinse water without added salt was used for both samples. In both cases, PAH-Py1 was first adsorbed onto the OTS surface at pH 9 without added salt for 30 min to make a uniform prime layer. It should be mentioned that only 1 min rinsing was applied to the first adhesion layer, avoiding serious desorption, but three thorough rinsing steps were applied for the following multilayer construction steps. During the subsequent assembly process, all of the polyelectrolyte solution pH values were fixed at 6.5. At pH 6.5, both PAH and PAA chains are substantially charged, causing adsorption of extended chains and producing thin films. By also fixing the pH of the rinsing solutions at 5.5−6.5, we attempted to exclude conformational variations due to pH and thus isolate the effect of salt concentration. To avoid long-term fluorescence quenching effects or slight changes in pH during assembly, we investigated multilayer construction up to three bilayers using fluorescence measurements.

Trace amounts of depleted PAH-Py1 in each step were measured by integrating the fluorescence spectra (350−650 nm) from adsorption and rinsing solutions after each step. All solutions were refreshed after each step, and the integrated values were normalized to the value obtained from the first PAA adsorption solution. Of the three 1 min rinsing steps, only the first rinse solutions were monitored for fluorescence. The relative amount of PAH-Py1 removed from the substrate surface at each assembly step shows a distinct dependence on salt conditions. A noteworthy result, shown in Figure 6, is

that the depletion of the first adsorbed PAH-Py1 chains was most severe in adsorption steps rather than in rinsing steps. In the assembly process following the adsorption of the PAH-Py prime layer, the adsorption time of subsequent layers was fixed at 15 min, which was much longer than the rinsing time of 1 min. This result indicates that the depletion process does not achieve an equilibrium state in the short time frame of the assembly steps. In this study, we tried to follow the typical assembly conditions to observe multilayer growth rather than to achieve equilibrium conditions like Izumrudov et al.;[52] thus, it should be kept in mind that changing the times allowed for adsorption and rinsing might cause additional variation in the multilayer growth. The result also shows that the adsorbed PAH-Py chains are seriously depleted from the hydrophobic surface due to increased segment charge repulsion and solvation or to ionic complexation in solution with the oppositely charged polyelectrolyte, PAA, during adsorption steps. This severe depletion was significantly suppressed when a salt was added into adsorption solutions as clearly shown in Figure 6 due to increased hydrophobic affinity to the surface. In Figure 6, the steps at $(0.5n + 0.5)$ are adsorption steps and those at $(0.5n + 0.75)$ are rinsing steps where $n = 0, 1, 2, ...$, and only the first PAH layer of the 0 bilayer is labeled. Thus, in the plot of fluorescence intensities normalized to the value of the second PAA solution (Figure 6), the decrease of the depleted amount with added salt indicates that the depletion in the subsequent solutions with added salt are remarkably small compared to the case of the solutions without added salt. The increase in ionic strength shields charged segments and enhances hydrophobic and van der Waals attractions between chains and the surface, causing a significant amount of the adsorbed chains to remain on the surface during adsorption and rinsing.

The coiling index measured from two different ionic strength cases also clearly shows the salt stabilization effect during adsorption (Figure S3). As described in the previous section, the coiling index of PAH-Py is drastically decreased after adsorption on the surface (coiling index $\sim$ 3). It is further decreased when the substrate is submerged into the subsequent PAA adsorption solutions (coiling index $\sim$ 1), which might originate from decreasing interpolymeric pyrene association due to depletion, PAH-Py chain extension or dissociation of pyrene aggregates during ionic complex formation of PAH-Py and PAA on the surface. A dramatic variation of the coiling index was observed after a three-bilayer assembly process. Without salt addition, the coiling index increased nearly up to the value in solution (coiling index $\sim$ 6), indicating that polymer chains adsorbed in a stretched form were assuming more coiled conformations again on the surface. In comparison, the chains maintained their extended conformations when 0.1 M NaCl salt was added into the subsequent PAH and PAA adsorption solutions (coiling index $\sim$ 2) although recoiling still occurs in a relatively small extent.

3.3.2. Multilayer Quality with Salt Stabilization. The two phenomena described in the previous sections in the no added salt regime—the conformational change of the adsorbed chains from an extended to a coiled state, and priming layer depletion during the assembly process—result in coagulation of ionic complexes on the surface upon multilayer formation. The chains do not keep their extended conformation on the surface without added salt, and effectively dewet and desorb, leaving coiled polymer chains on the surface. These chains form ionic complexes with the incoming counter polyelectrolytes during multilayer adsorption; thus, after building up many bilayers, the final surface morphology becomes rougher, forming domains of ionic aggregates rather than flat multilayers. The AFM topography of $(PAH/PAA)_{3.5}$ assembled at pH 6.5/6.5 without added salt on raised areas of PDMS stamps (Figure 7a in height mode and Figure 7b in phase mode) shows such a surface morphology which has developed due to coiling and desorption. After only a 3.5 bilayer assembly, the bare PDMS surface becomes exposed and the height of the polyelectrolyte aggregates on the surface is around 67 nm on average and the rms roughness is 16.2 nm. This instability of polyelectrolyte thin films becomes more marked after assembling additional bilayers. For $(PAH/PAA)_{10.5}$ assembled at the same conditions, a larger area of bare PDMS surface is exposed, presenting tiny islands of polyelectrolyte aggregates with 25 nm height on the surface and 6.5 nm rms roughness, as shown in Figure 7e,f.

With salt stabilization, the resulting polyelectrolyte multilayers become less coagulated. In the case of $(PAH/PAA)_{3.5}$ assembled at pH 6.5/6.5 with 0.1 M NaCl, the coiling and dewetting behavior is significantly suppressed because of increased ionic strength. AFM images (Figure 7c in height mode and Figure 7d in phase mode) show a flat surface with an rms roughness of 4.4 nm, consistent with the coiling index variation described in the previous section. Although there is significant morphological evolution after 10.5 bilayer assembly at the conditions that lead to a very rough multilayer (45 nm rms roughness), a less exposed PDMS surface is found for this film than the one formed without salt, and the morphology is regular with about 160 nm height, as seen in Figure 7g,h.

While multilayers could uniformly be formed with salt stabilization, high ionic strength is not the only factor that guarantees uniform multilayer formation. The hydrophobicity of the polyelectrolytes plays an important role in the resulting multilayer quality, and multilayer formation would be possible without added salt if all of the polyelectrolytes employed were strongly hydrophobic, as reported by Delcorte and Bertrand.[32] In comparison, as shown in this study, the use of a hydrophilic polyanion, PAA, seems to make the formed multilayer less stable, causing the evolution of a rough morphology as the number of layers increases.

The development of domainlike polyelectrolyte coagulates observed when we use polyelectrolytes with pH-dependent degrees of ionization might be explained by dewetting theories of thin liquid films. On a nonwettable surface, thin liquid films can be dewet via nucleation and growth or spinodal decomposition mechanisms.[53] In this work, we could observe a morphology evolved through spinodal decomposition in $(PAH/PAA)_{10.5}$ assembled at pH 7.5/3.5 without added salt (Figure 7i, 21 nm rms roughness). In a specific example of polystyrene thin films on a silicon substrate,[54] the thin films broke up due to the amplification of thermal fluctuations and phase separation and evolved to form wrinkled and coarsened patterns, which were elucidated using a capillary wave instability model. We think that a similar theoretical treatment can be applied to multilayer thin

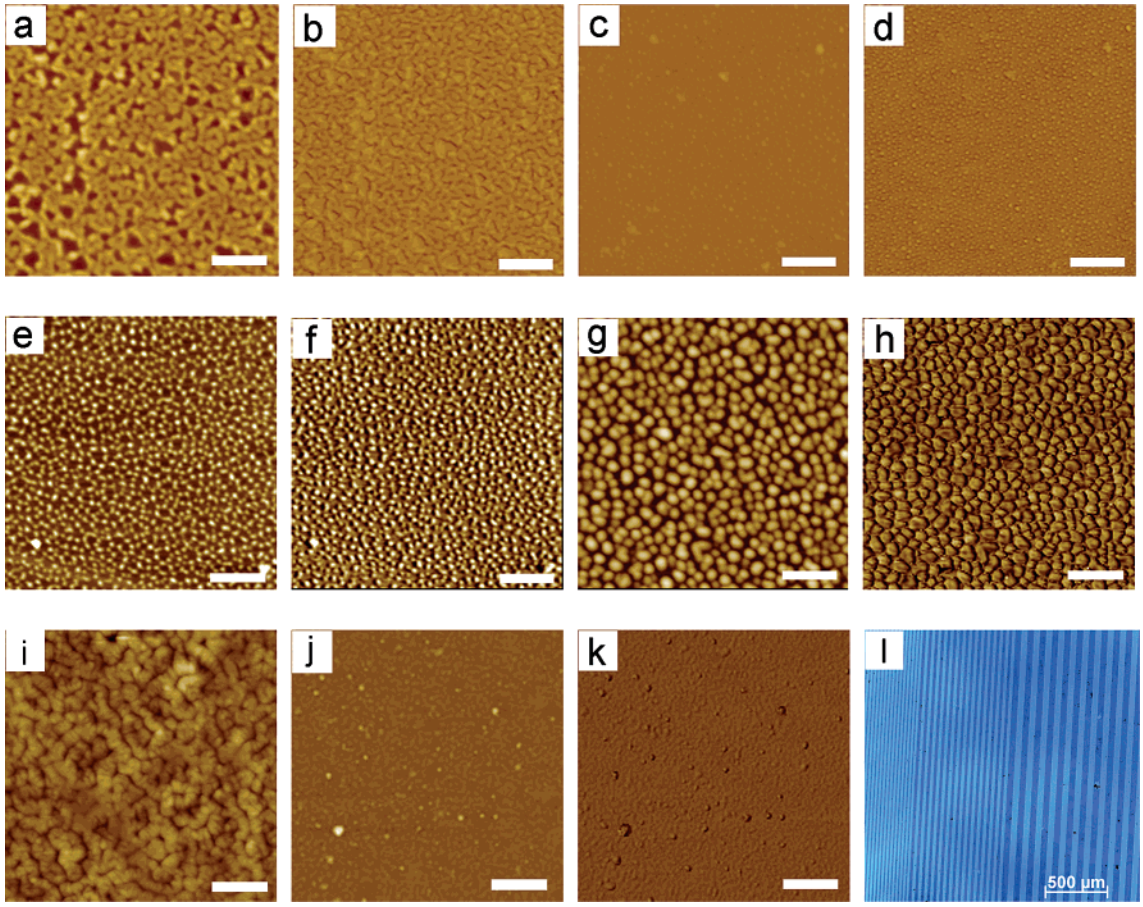

Figure 7. All films shown were constructed on a PAH base layer adsorbed at pH 9.0. AFM images of $(PAH/PAA)_{3.5}$ (no added salt, pH 6.5/6.5) (a) in height mode and (b) in phase mode; $(PAH/PAA)_{3.5}$ (0.1 M NaCl, pH 6.5/6.5) (c) in height mode and (d) in phase mode; $(PAH/PAA)_{10.5}$ (no added salt, pH 6.5/6.5) (e) in height mode and (f) in phase mode; $(PAH/PAA)_{10.5}$ (0.1 M NaCl, pH 6.5/6.5) (g) in height mode and (h) in phase mode; (i) $(PAH/PAA)_{10.5}$ (no added salt, pH 7.5/3.5) in height mode; $PAH/(SPS/PDAC)_{10.5}$ (0.1 M NaCl, pH 5.5/5.5) (j) in height mode and (k) in phase mode. All multilayers were assembled on PDMS stamps with micropatterned lines, and AFM images were scanned for the multilayers on positive motifs. The scan size of all images is 10 × 10 μm^2, and the length of scale bar is 2 μm. The z range is 200 nm for (a−d) and 520 nm for (d−k). (l) An optical microscope image of transfer-patterned $PAH/(SPS/PDAC)_{10.5}$, taken in a reflection mode.

films to explain the phenomena in Figure 7a−i, a study which is ongoing.

A flat and smooth multilayer without surface roughening was obtained with salt stabilization when we combined a weak PAH base layer with a hydrophobic strong polyion pair as shown in Figure 7j,k. In this example, a $PAH/(SPS/PDAC)_{10.5}$ multilayer was built up at pH 5.5/5.5 with 0.1 M NaCl on a PDMS stamp, resulting in no morphological evolution and 5.4 nm rms roughness. Transfer-printed line patterns of $PAH/(SPS/PDAC)_{10.5}$ assembled with salt stabilization are shown in an optical microscope image in Figure 7l. It is clear that the combination of (a) achieving a uniform hydrophobic weak polyelectrolyte base layer (as in Figure 7c,d) and (b) using a more hydrophobic polyion pair can lead to highly uniform, stable film.

It is noted that film stability on neutral hydrophobic surface is extremely sensitive to process conditions such as substrate orientation, rinse times, and exposure to shear flow during adsorption; here we observe the more challenging condition of a lateral surface that may undergo some shear on dipping.

Stabilization with differing salt concentrations was investigated by building up multilayers of SPS and PDAC on our PAH-coated neutral hydrophobic surface and by measuring QCM. In varying NaCl concentrations from 0 to 0.4 M, the regular growth of multilayers appears when 0.1 and 0.2 M NaCl were added into polyelectrolyte solutions, which is typical with strong polyelectrolytes with added electrolytes,[55,56] but at conditions of 0, 0.3, and 0.4 M NaCl, we did not observe regular growth of multilayers (Figure S4). This results show that multilayering of the polyelectrolytes on the surface utilizing weak short-range interactions is possible only in a narrow salt range, different from that on a charged surface.[52,55]

4. Conclusion

The mechanism of multilayer growth of polyelectrolytes on a neutral hydrophobic surface has been investigated by observing the conformational and depletion behaviors of the first adhesion layer of a weak polyelectrolyte, PAH, on the surface during assembly processes, and the behavior has been compared to the final quality of the resulting multilayer thin films. Ellipsometry experiments and the variation of coiling index of a polymer chain measured by using pyrene-labeled PAH revealed that a hydrophobic weak polyelectrolyte can adsorb onto a neutral hydrophobic surface, forming a densely packed uniform adhesion layer, and that polymer chains with compact globular shape in solution were adsorbed on the surface in an extended chain conformation. The amount of the adsorbed polyelectrolyte increased with solution pH, and the increased

concentration of an added electrolyte caused a thinner layer by shielding repulsive interactions and enhancing hydrophobic attractions of the adsorbed chains to the surface, verifying the theory proposed by Dobrynin and Rubinstein. This salt stabilization also affected subsequent multilayer formation on the PAH primary layer. Without an added electrolyte in the polyelectrolyte solutions, the first adhesion layer was seriously depleted, and the extended chains on the surface recoiled and dewet during the assembly process, causing the development of coagulated polyelectrolyte structures. On the other hand, uniform and flat multilayer thin films could be formed on the surface with an added electrolyte. For multilayers that grew regularly on the surface, the concentration of the added electrolyte had a narrower window than on a charged surface.

Future directions of this work involve applying MTP to practical device fabrications and include a theoretical characterization of the instability of the muitilayer thin films as a function of assembly conditions. Using the principles found in this study, nanocomposite thin films including various kinds of charged materials such as electroluminescent and electrochromic nanocrystals, biofunctional molecules, or functional polyelectrolytes can be formed on a neutral hydrophobic PDMS surface. We anticipate that the transfer printing of these thin film patterns will accelerate the development of devices utilizing LBL multilayer thin films with simple processing.

Acknowledgment. The authors thank Dr. Sungjee Kim and Dr. Sang-Wook Kim for their help with fluorescence spectroscopy experiments, Professor Rubner and Mr. Daeyeon Lee at MIT for their permission and help with QCM experiments, Professor Dobrynin at University of Connecticut for his comment about applicability of his theory to the case in this study, and Dr. Geoffrey Lowman for careful review of this manuscript. This work was supported by the MRSEC program of the National Science Foundation under Award DMR 02-13282 and by the Army Research Office-funded Institute for Soldier Nanotechnologies at MIT.

Supporting Information Available: Description of fluorescence characteristics, characterization of PAH-Py in solutions, adsorption theory of hydrophobic polyelectrolytes at neutral hydrophobic surfaces, coiling index variation during multilayer assembly, and frequency shift of QCM during multilayer assembly. This material is available free of charge via the Internet at http://pubs.acs.org.

References and Notes

(1) Decher, G.; Hong, J. D. *Makromol. Chem. Macromol. Symp.* **1991**, *46*, 321.
(2) Iler, R. K. *J. Colloid Interface Sci.* **1966**, *21*, 569.
(3) Zhang, L. M.; Zhang, F. J.; Wang, Y. Q.; Claus, R. O. *J. Chem. Phys.* **2002**, *116*, 6297.
(4) Schrof, W.; Rozouvan, S.; Van Keuren, E.; Horn, D.; Schmitt, J.; Decher, G. *Adv. Mater.* **1998**, *10*, 338.
(5) Fou, A. C.; Rubner, M. F. *Macromolecules* **1995**, *28*, 7115.
(6) Cheung, J. H.; Fou, A. F.; Rubner, M. F. *Thin Solid Films* **1994**, *244*, 985.
(7) Wang, Y.; Tang, Z. Y.; Correa-Duarte, M. A.; Liz-Marzan, L. M.; Kotov, N. A. *J. Am. Chem. Soc.* **2003**, *125*, 2830.
(8) Gao, M. Y.; Richter, B.; Kirstein, S. *Adv. Mater.* **1997**, *9*, 802.
(9) Clark, S. L.; Handy, E. S.; Rubner, M. F.; Hammond, P. T. *Adv. Mater.* **1999**, *11*, 1031.
(10) DeLongchamp, D. M.; Hammond, P. T. *Chem. Mater.* **2004**, *16*, 4799.
(11) DeLongchamp, D. M.; Hammond, P. T. *Adv. Mater.* **2001**, *13*, 1455.
(12) Schlenoff, J. B.; Laurent, D.; Ly, H.; Stepp, J. *Adv. Mater.* **1998**, *10*, 347.
(13) Cutler, C. A.; Bouguettaya, M.; Reynolds, J. R. *Adv. Mater.* **2002**, *14*, 684.
(14) Tokuhisa, H.; Hammond, P. T. *Adv. Funct. Mater.* **2003**, *13*, 831.
(15) He, J. A.; Mosurkal, R.; Samuelson, L. A.; Li, L.; Kumar, J. *Langmuir* **2003**, *19*, 2169.
(16) Li, L. S.; Jia, Q. X.; Li, A. D. Q. *Chem. Mater.* **2002**, *14*, 1159.
(17) Berg, M. C.; Yang, S. Y.; Hammond, P. T.; Rubner, M. F. *Langmuir* **2004**, *20*, 1362.
(18) Kim, H.; Doh, J.; Irvine, D. J.; Cohen, R. E.; Hammond, P. T. *Biomacromolecules* **2004**, *5*, 822.
(19) Tryoen-Toth, P.; Vautier, D.; Haikel, Y.; Voegel, J. C.; Schaaf, P.; Chluba, J.; Ogier, J. *J. Biomed. Mater. Res.* **2002**, *60*, 657.
(20) Mendelsohn, J. D.; Yang, S. Y.; Hiller, J.; Hochbaum, A. I.; Rubner, M. F. *Biomacromolecules* **2003**, *4*, 96.
(21) Khopade, A. J.; Caruso, F. *Biomacromolecules* **2002**, *3*, 1154.
(22) Zhu, H. G.; Ji, J.; Tan, Q. G.; Barbosa, M. A.; Shen, J. C. *Biomacromolecules* **2003**, *4*, 378.
(23) Park, J.; Hammond, P. T. *Adv. Mater.* **2004**, *16*, 520.
(24) Lutkenhaus, J. L.; Hrabak, K.; McEnnis, K.; Hammond, P. T. *J. Am. Chem. Soc.*, in press.
(25) Mamedov, A.; Kotov, N.; Prato, M.; Guldi, D.; Wicksted, J.; Hirsch, A. *Nat. Mater.* **2002**, *1*, 190.
(26) Yoo, P. J.; Nam, K. T.; Qi, J.; Lee, S.-K.; Park, J.; Belcher, A.; Hammond, P. T., to be submitted.
(27) von Klitzing, R.; Tieke, B. *Adv. Polym. Sci.* **2004**, *165*, 177.
(28) Kotov, N. *Nat. Mater.* **2004**, *3*, 669.
(29) Jiang, C.; Markutsya, S.; Tsukruk, V. *Adv. Mater.* **2004**, *16*, 157.
(30) Nolte, A. J.; Rubner, M. F.; Cohen, R. E. *Macromolecules* **2005**, *38*, 5367.
(31) Roberts, M. J.; Lindsay, G. A.; Herman, W. N.; Wynne, K. J. *J. Am. Chem. Soc.* **1998**, *120*, 11202.
(32) Delcorte, A.; Bertrand, P.; Wischerhoff, E.; Laschewsky, A. *Langmuir* **1997**, *13*, 5125.
(33) Kramer, G.; Buchhammer, K.; Lunkwitz, K. *Colloids Surf. A* **1997**, *122*, 1.
(34) Dobrynin, A. V.; Deshkovski, A.; Rubinstein, M. *Macromolecules* **2001**, *34*, 3421.
(35) Dobrynin, A. V.; Rubinstein, M. *J. Phys. Chem. B* **2003**, *107*, 8260.
(36) Dobrynin, A. V.; Rubinstein, M. *Macromolecules* **2002**, *35*, 2754.
(37) Dobrynin, A. V.; Deshkovski, A.; Rubinstein, M. *Phys. Rev. Lett.* **2000**, *84*, 3101.
(38) Dobrynin, A. V.; Rubinstein, M. *Macromolecules* **1999**, *32*, 915.
(39) Chandar, P.; Somasundaran, P.; Turro, N. J.; Waterman, K. C. *Langmuir* **1987**, *3*, 298.
(40) Winnik, M. A.; Bystryak, S. M.; Liu, Z. Q.; Siddiqui, J. *Macromolecules* **1998**, *31*, 6855.
(41) Winnik, F. M. *Chem. Rev.* **1993**, *93*, 587.
(42) Anghel, D. F.; Alderson, V.; Winnik, F. M.; Mizusaki, M.; Morishima, Y. *Polymer* **1998**, *39*, 3035.
(43) Kramer, G.; Somasundaran, P. *Langmuir* **2002**, *18*, 9357.
(44) Nezu, T.; Winnik, F. M. *Biomaterials* **2000**, *21*, 415.
(45) Chodanowski, P.; Stoll, S. *J. Chem. Phys.* **1999**, *111*, 6069.
(46) Kiriy, A.; Gorodyska, G.; Minko, S.; Jaeger, W.; Stepanek, P.; Stamm, M. *J. Am. Chem. Soc.* **2002**, *124*, 13454.
(47) Carbaja-Tinoco, M. D.; Ober, R.; Dolbnya, I.; Bras, W.; Williams, C. E. *J. Phys. Chem. B* **2002**, *106*, 12165.
(48) Jiang, X. Ph.D. Thesis, Department of Chemical Engineering, MIT, 2002.
(49) Borisov, O. V.; Hakem, F.; Vilgis, T. A.; Joanny, J. F.; Johner, A. *Eur. Phys. J. E* **2001**, *6*, 37.
(50) Poncet, C.; Tiberg, F.; Audebert, R. *Langmuir* **1998**, *14*, 1697.
(51) Tamashiro, M. N.; Hernandez-Zapata, E.; Schorr, P. A.; Balastre, M.; Tirrell, M.; Pincus, P. *J. Chem. Phys.* **2001**, *115*, 1960.
(52) Izumrudov, V.; Kharlampieva, E.; Sukhishvili, S. A. *Macromolecules* **2004**, *37*, 8400.
(53) Wyart, F. B.; Daillant, J. *Can. J. Phys.* **1990**, *68*, 1084.
(54) Xie, R.; Karim, A.; Douglas, J. F.; Han, C. C.; Weiss, R. A. *Phys. Rev. Lett.* **1998**, *81*, 1251.
(55) Clark, S. L.; Montague, M. F.; Hammond, P. T. *Macromolecules* **1997**, *30*, 7237.
(56) McAloney, R. A.; Sinyor, M.; Dudnik, V.; Goh, M. C. *Langmuir* **2001**, *17*, 6655.

MA051158C